A *pex1* missense mutation improves peroxisome function in a subset of *Arabidopsis pex6* mutants without restoring PEX5 recycling

Kim L. Gonzalez[a,1], Sarah E. Ratzel[a], Kendall H. Burks[a,2], Charles H. Danan[a,3], Jeanne M. Wages[a,4], Bethany K. Zolman[a,b], and Bonnie Bartel[a,5]

[a]Department of Biosciences, Rice University, Houston, TX 77005; and [b]Department of Biology, University of Missouri–St. Louis, St. Louis, MO 63121

Contributed by Bonnie Bartel, February 20, 2018 (sent for review December 11, 2017; reviewed by Alison Baker and Jianping Hu)

Peroxisomes are eukaryotic organelles critical for plant and human development because they house essential metabolic functions, such as fatty acid β-oxidation. The interacting ATPases PEX1 and PEX6 contribute to peroxisome function by recycling PEX5, a cytosolic receptor needed to import proteins targeted to the peroxisomal matrix. *Arabidopsis pex6* mutants exhibit low PEX5 levels and defects in peroxisomal matrix protein import, oil body utilization, peroxisomal metabolism, and seedling growth. These defects are hypothesized to stem from impaired PEX5 retrotranslocation leading to PEX5 polyubiquitination and consequent degradation of PEX5 via the proteasome or of the entire organelle via autophagy. We recovered a *pex1* missense mutation in a screen for second-site suppressors that restore growth to the *pex6-1* mutant. Surprisingly, this *pex1-1* mutation ameliorated the metabolic and physiological defects of *pex6-1* without restoring PEX5 levels. Similarly, preventing autophagy by introducing an *atg7*-null allele partially rescued *pex6-1* physiological defects without restoring PEX5 levels. *atg7* synergistically improved matrix protein import in *pex1-1 pex6-1*, implying that *pex1-1* improves peroxisome function in *pex6-1* without impeding autophagy of peroxisomes (i.e., pexophagy). *pex1-1* differentially improved peroxisome function in various *pex6* alleles but worsened the physiological and molecular defects of a *pex26* mutant, which is defective in the tether anchoring the PEX1–PEX6 hexamer to the peroxisome. Our results support the hypothesis that, beyond PEX5 recycling, PEX1 and PEX6 have additional functions in peroxisome homeostasis and perhaps in oil body utilization.

peroxisome | peroxin | pexophagy | AAA ATPase | oil bodies

Plants and animals can store fixed carbon as triacylglycerol (TAG), which can then be mobilized when energy is required. *Arabidopsis* seedling germination and early growth are fueled by breakdown of TAG stored in oil bodies via fatty acid β-oxidation in peroxisomes, single membrane-bound organelles. During germination, fatty acids hydrolyzed from TAG are activated with CoA before import through the peroxisomal ABC transporter PXA1 (1). In the peroxisome, fatty acids undergo β-oxidation to acetyl-CoA, which ultimately can be converted to sucrose. If germinating seedlings inefficiently catabolize fatty acids, growth is impeded. However, growth can be restored by providing sucrose in the medium (reviewed in ref. 2). In addition to fatty acid β-oxidation, plant peroxisomes host various other oxidative reactions (reviewed in refs. 3 and 4), including conversion of the protoauxin indole-3-butyric acid (IBA) to the active auxin indole-3-acetic acid (IAA; reviewed in ref. 5). The IAA generated following IBA treatment inhibits root elongation and promotes lateral root formation in WT, and mutants with dysfunctional β-oxidation enzymes or impaired import of these enzymes into the organelle often display decreased IBA responsiveness (reviewed in ref. 2).

Peroxisomal enzymes are posttranslationally imported into the organelle. Peroxisomal matrix proteins are recognized in the cytosol by the receptors PEX5 and PEX7, which bind proteins harboring one of two peroxisomal targeting signals (PTSs). PEX5 recognizes a C-terminal PTS1 (6), and PEX7 recognizes a PTS2 near the N terminus (7). These receptor–cargo complexes dock with peroxisomal membrane proteins, PEX13 and PEX14 (reviewed in ref. 8), and PEX14 is thought to aid PEX5 in forming a dynamic pore through which cargo is translocated to the matrix (9). Following cargo release, yeast PEX5 in the peroxisomal membrane (10) is ubiquitinated by PEX4 (11, 12) and the RING complex peroxins (PEX2, PEX10, and PEX12) (13) and then retrotranslocated to the cytosol with the assistance of the PEX1–PEX6 ATPase complex (14), which is tethered to the peroxisome by PEX15 in yeast (15) and PEX26 in mammals (16) and plants (17). When PEX5 is inefficiently retrotranslocated (as in *pex1* or *pex6* mutants), PEX5 is polyubiquitinated, which can trigger degradation of PEX5 by the proteasome (18, 19) or degradation of the entire organelle via specialized autophagy (i.e., pexophagy) (20).

PEX1 and PEX6 are type II AAA proteins (ATPases Associated with various cellular Activities) with two AAA domains. These domains generally include Walker A and Walker B motifs,

Significance

ATPases have diverse cellular roles, including extracting proteins from membranes to maintain organellar function. The PEX1–PEX6 heterohexameric ATPases are thought to retrotranslocate PEX5 from the peroxisome membrane, and PEX1–PEX6 dysfunction impairs peroxisome biogenesis in humans and plants. We implemented a *pex6* suppressor screen in *Arabidopsis* and recovered a compensatory *pex1* allele that rescues several *pex6* defects. Preventing autophagy also improved *pex6* peroxisome function, and combining the *pex1* and autophagy lesions delivered synergistic benefits. Surprisingly, these different alterations ameliorated *pex6* symptoms without notably restoring the sole known function of PEX6, suggesting that PEX1–PEX6 has unexplored functions. Because the *pex6* mutations ameliorated by *pex1* are analogous to those in human *pex6* patients, this study informs research on peroxisome dysfunction in other eukaryotes.

Author contributions: K.L.G., S.E.R., B.K.Z., and B.B. designed research; K.L.G., S.E.R., K.H.B., C.H.D., J.M.W., and B.K.Z. performed research; K.L.G., S.E.R., J.M.W., B.K.Z., and B.B. analyzed data; and K.L.G. and B.B. wrote the paper.

Reviewers: A.B., University of Leeds; and J.H., Michigan State University.

The authors declare no conflict of interest.

[1]Present address: Biology Department, Stanford University, Stanford, CA 94305.

[2]Present address: Washington University School of Medicine in St. Louis, St. Louis, MO 63130.

[3]Present address: Perelman School of Medicine, University of Pennsylvania, Philadelphia, PA 19104.

[4]Present address: Biotechnology Program, Bluegrass Community and Technical College, Lexington, KY 40506.

[5]To whom correspondence should be addressed. Email: bartel@rice.edu.

This article contains supporting information online at www.pnas.org/lookup/suppl/doi:10.1073/pnas.1721279115/-/DCSupplemental.

Published online March 19, 2018.

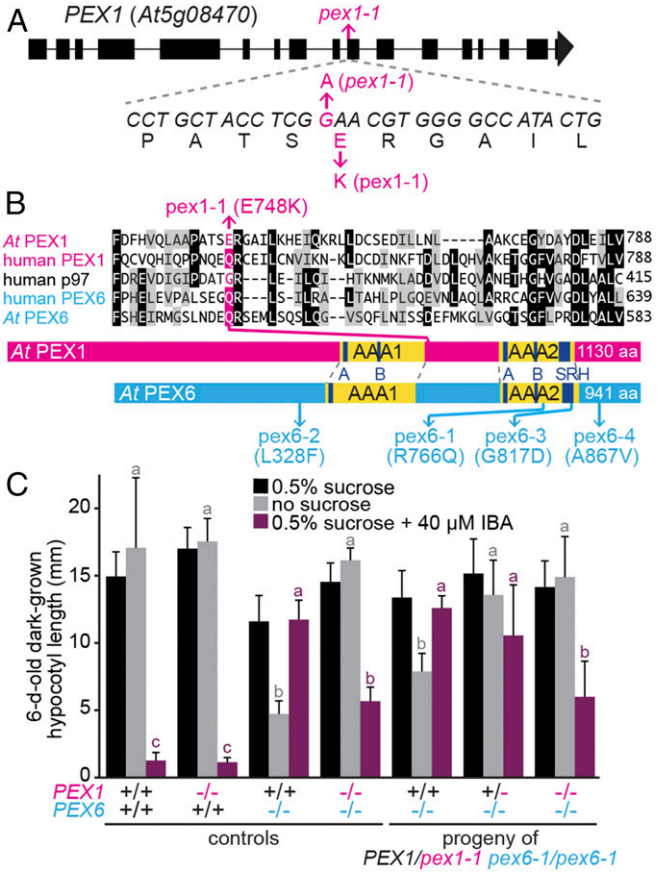

Fig. 1. *pex1-1* identification. (*A*) *PEX1* gene diagram showing exons (rectangles), introns (lines), and the location of *pex1-1*, a G-to-A transition that yields a Glu748-to-Lys substitution. (*B*) Partial alignment of *Arabidopsis* and human PEX1 and PEX6 and human p97 (a related ATPase) above protein schematic illustrations depicting the locations of *pex1-1* and previously described *pex6* missense alleles (35, 37, 44). The complete AAA domains are in yellow, with the Walker A (*A*), Walker B (*B*), and second region of homology (SRH) domains highlighted in navy blue. (*C*) *pex1-1* is semidominant; the *PEX1/pex1-1* heterozygote partially suppresses *pex6-1* sucrose dependence and IBA resistance. Seedlings were grown on the indicated media for 1 d under yellow-filtered light before moving to darkness for 5 d. Bars indicate mean hypocotyl lengths, and error bars indicate SD ($n \geq 13$ except for *pex6-1 PEX1* and *pex6-1 pex1-1* from the segregating parent, for which $n \geq 5$). Means not sharing a letter above the bar are significantly different as determined by one-way ANOVA ($P < 0.001$).

but the PEX6 AAA1 domain lacks a canonical Walker B motif and is unable to hydrolyze ATP (reviewed in ref. 21). *Saccharomyces cerevisiae* PEX1 and PEX6 form a heterohexamer (22) of alternating subunits (23–25). Biochemical experiments (26) indicate that PEX1–PEX6 can thread client proteins through a central pore revealed in structural studies (23–25, 27). Intriguingly, PEX15 is not only a tether (15), but PEX15 lacking its C-terminal transmembrane domain is an in vitro client of the ATPase (26). Human PEX1 also forms a PEX5-interacting homotrimer in the cytosol (28) that may modulate cytosolic PEX5 homooligomerization (29). Moreover, overexpressing *PEX6* in yeast suppresses the import defects of a mitochondrial ATPase missense mutation (30), suggesting that PEX6 may also function beyond peroxisomes.

In humans, the generally fatal peroxisomal biogenesis disorders (PBDs) are caused by mutations in various *PEX* genes, most often *PEX1* and *PEX6* (reviewed in ref. 31). *Arabidopsis* PEX1 and PEX6 are 28% and 33% identical at the amino acid level with human PEX1 and PEX6, respectively, and appear to function similarly to their human counterparts (32–34). For example, expressing a human *PEX6* cDNA rescues an *Arabidopsis pex6* mutant (35), and like human PBD patients with dysfunctional PEX6 (36), several *Arabidopsis pex6* mutants have low PEX5 levels (35, 37). Moreover, three of the six reported *Arabidopsis pex1* (38) or *pex6* (35, 37) missense alleles are equivalent to causal mutations in patients with PBD (www.dbpex.org/home.php) (39–41).

The peroxisomal ATPase complex is also vital for plants. *Arabidopsis PEX1*- (42) and *PEX26*- (17, 43) null alleles confer embryo lethality, and the *pex1-3* missense allele is lethal when homozygous (38). *pex1-3* and *pex1-2* alter conserved AAA2 residues, and *PEX1*/*pex1-3* and *pex1-2* plants display β-oxidation and matrix protein import defects (38). Moreover, *pex1-2* has decreased PEX1 and PEX6 levels, suggesting that this allele confers instability to the complex. The *pex6-1*, *pex6-3*, and *pex6-4* missense mutations also lie in or near the AAA2 domain (Fig. 1*B* and Fig. S1) and result in small pale green plants with β-oxidation defects and low PEX5 levels (35, 37). In contrast, the mild *pex6-2* allele lies N-terminal to the AAA1 domain (Fig. 1*B*), lacks notable β-oxidation defects, complements *pex6-1* (44), and displays elevated PEX5 levels (37). The two viable *pex26* mutants, *pex26-1* (37) and *aberrant peroxisome morphology9* (*apem9*) (17), display distinct phenotypes as well. *apem9-1* is a mild missense allele that lacks notable β-oxidation defects and has matrix protein import defects only in a subset of tissues (17), whereas the *pex26-1* splice-site mutation confers seedling β-oxidation defects and clustered peroxisomes (37). Lipid droplets accumulate in *PEX5*$^{-/-}$ mouse hepatocytes (45), and oil bodies persist during *pex6-1*, *pex6-3*, *pex6-4*, and *pex26-1* seedling development after oil bodies have been consumed in WT (37), indicating that the peroxisome retrotranslocation machinery directly or indirectly promotes oil body utilization. Finally, increasing PEX5 levels in *pex6-1*, *pex6-3*, *pex6-4*, and *pex26-1* has disparate effects. Excess PEX5 restores growth and oil body utilization in *pex6-1* and *pex6-3* but not in *pex6-4* or *pex26-1* (37), hinting that PEX5 recycling is not the sole function of the peroxisomal ATPase.

To learn more about peroxisomal ATPase complex functions, we employed a forward-genetic suppressor screen of *Arabidopsis pex6-1* and recovered a missense mutation in *PEX1* (*pex1-1*) that restored *pex6-1* growth without an exogenous fixed carbon source. Moreover, we found that preventing autophagy also partially ameliorated *pex6-1* defects. Rescue of *pex6-1* by *pex1-1* was more effective than preventing autophagy or reducing *PEX13* expression, which also improves *pex6-1* peroxisomal function (46). To explore the specificity of *pex6* restoration, we characterized a suite of *pex1* double mutants, and found that *pex1-1* improved several physiological and molecular defects in a subset of *pex6* mutants while worsening a *pex26* mutant. Surprisingly, *pex1-1* amelioration of *pex6* physiological defects was not accompanied by restored PEX5 levels, supporting the hypothesis that PEX1 and PEX6 have roles beyond PEX5 recycling.

Results

The *pex1-1* Missense Mutation Improves *pex6-1* Growth. We sought to elucidate functions of the peroxisomal ATPase complex by identifying genes that genetically interact with *PEX6*. Given previous demonstrations that elevating *PEX5* or decreasing *PEX13* expression ameliorates some physiological defects of the *pex6-1* missense allele (35, 46), we screened for *pex6-1* suppressors. Like other *Arabidopsis pex* mutants (47–53), *pex6-1* displays impaired growth on medium lacking sucrose (35), providing a facile screen for suppressors with increased growth. We mutagenized *pex6-1* seeds with ethyl methanesulfonate (EMS) and selected dark-grown M_2 seedlings with longer hypocotyls than *pex6-1* on medium lacking sucrose. One suppressor that restored *pex6-1* growth and partially restored IBA responsiveness was retained for further analysis.

After backcrossing to the *pex6-1* parent, we sequenced genomic DNA from the suppressor (Fig. S2) and found a mutation in *PEX1* (Fig. 1*A*). This G4127-to-A transition in exon 10 causes a glutamic acid to lysine (E748K) change (Fig. 1*A*) in the region between the two AAA domains (Fig. 1*B*). We named this allele *pex1-1*. Unlike *pex6-1*, the *pex1-1* single mutant grew similarly to

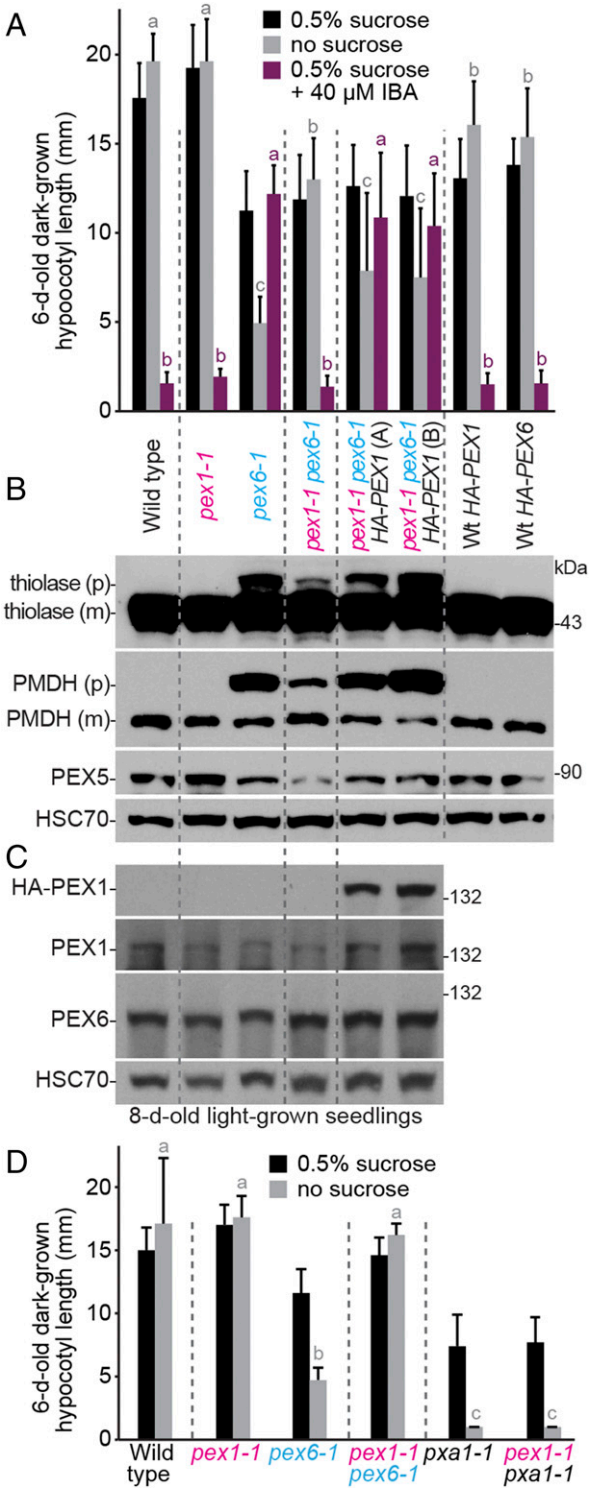

Fig. 2. Overexpressing *PEX1* in *pex1-1 pex6-1* phenocopies *pex6-1* defects; *pex1-1* does not restore *pxa1-1* growth. (*A*) Expressing *HA-PEX1* increases resistance to the inhibitory effects of IBA and hypocotyl elongation dependence on exogenous sucrose of dark-grown *pex1-1 pex6-1* seedlings. Two independent *pex1-1 pex6-1 35S:HA-PEX1* lines (*A* and *B*) are shown. Seedlings were grown as in the legend to Fig. 1*C*. Bars indicate mean hypocotyl lengths ($n \geq 13$), and error bars indicate SD. (*B*) PTS2-processing defects of light-grown *pex1-1 pex6-1* seedlings are worsened by *HA-PEX1* expression. An immunoblot of 8-d-old light-grown seedling extracts was serially probed with antibodies to the indicated proteins. For thiolase and PMDH, precursor (p) and mature (m) proteins are indicated. (*C*) PEX1 and PEX6 levels resemble WT levels in *pex1-1*. An immunoblot of 8-d-old light-grown seedling extracts was serially probed with antibodies to the indicated proteins. For *B* and *C*, the positions of molecular mass markers (in kilodaltons) are indicated on the right and HSC70 is a loading control. (*D*) *pex1-1* does not improve growth of *pxa1-1* seedlings in the absence of sucrose. Seedlings were grown as in the legend to Fig. 1*C*. Bars indicate mean hypocotyl lengths ($n \geq 13$), and error bars indicate SD. In *A* and *D*, means not sharing a letter above the bar are significantly different as determined by one-way ANOVA ($P < 0.001$).

WT on IBA or with and without sucrose (Fig. 1*C*), suggesting that *pex1-1* did not markedly affect peroxisome function when *PEX6* was WT. Moreover, PEX1 and PEX6 levels were similar to WT levels in the single and double mutants (Fig. 2*C*), indicating that *pex1-1* did not notably affect stability of the ATPase hexamer components. Suppression was linked to *PEX1*; growth of suppressor backcross progeny on medium containing IBA or lacking sucrose correlated with *pex1-1* inheritance (Fig. 1*C*). Moreover, *pex1-1*$^{+/-}$ *pex6-1*$^{-/-}$ seedlings displayed intermediate suppression between homozygous *PEX1*$^{+/+}$ *pex6-1*$^{-/-}$ and *pex1-1*$^{-/-}$ *pex6-1*$^{-/-}$ phenotypes (Fig. 1*C*), indicating semidominance. To determine whether *pex1-1* was the causal lesion suppressing *pex6-1*, we expressed *HA-PEX1* from the constitutive *35S* cauliflower mosaic virus promoter in *pex1-1 pex6-1*. We found that dark-grown *pex1-1 pex6-1* seedlings expressing *HA-PEX1* displayed reduced hypocotyl elongation without sucrose and increased IBA resistance, similar to *pex6-1* (Fig. 2*A*).

Physiological defects of *pex* mutants are often ascribed to matrix protein import defects (48, 50–53), and the proteolytic processing of PTS2 proteins that occurs after import (54) can be used as an import proxy. We found that the *pex1-1* mutant fully processed PTS2 proteins and partially restored PTS2 processing of thiolase and PMDH in *pex6-1* (Fig. 2*B*). Moreover, expressing *HA-PEX1* decreased thiolase and PMDH processing in *pex1-1 pex6-1* (Fig. 2*B*). Because expressing *HA-PEX1* in *pex1-1 pex6-1* counteracted the beneficial effects of *pex1-1* (Fig. 2 *A* and *B*), we concluded that the identified *pex1-1* mutation was the causal *pex6-1* suppressor.

***pex1-1* Effects Are Specific to the PEX1–PEX6–PEX26 Complex.** To determine if the *pex1-1* lesion improved peroxisome function in general, we crossed *pex1-1* to *pxa1-1,* which is impaired in the peroxisomal transporter that moves β-oxidation substrates into the peroxisome (55). *pex1-1* did not significantly restore *pxa1-1* growth on medium without sucrose (Fig. 2*D*), indicating that *pex1-1* did not improve *pex6-1* seedling growth by bypassing the requirement for peroxisomal fatty acid β-oxidation.

To examine the specificity of the *pex1-1* suppression among *pex6* alleles, we compared peroxisome function of *pex1-1 pex6-1* to double mutants of *pex1-1* with *pex6-2* (44), *pex6-3* (37), and *pex6-4* (37). Intriguingly, *pex1-1* did not similarly suppress all *pex6* mutants. In addition to improving growth without sucrose, *pex1-1* increased sensitivity of *pex6-1* dark-grown hypocotyls to IBA (Fig. 3*A*) and slightly increased *pex6-1* hypocotyl sensitivity to the IBA analog 2,4-dichlorophenoxybutyric acid (2,4-DB) (Fig. 3*B*). Similarly, *pex1-1* rescued *pex6-3* physiological defects, largely restoring IBA and 2,4-DB responsiveness and the ability to grow without sucrose in the dark (Fig. 3 *A* and *B*). Although *pex1-1* did not significantly improve IBA-induced lateral rooting in *pex6-1*, *pex1-1* largely restored the ability of *pex6-3* to respond to IBA in this assay (Fig. 3*C*). Aside from a partial restoration of growth without sucrose in *pex1-1 pex6-4* (Fig. 3*A*), *pex1-1* did not significantly alter hypocotyl IBA (Fig. 3*A*) or 2,4-DB (Fig. 3*B*) responsiveness or IBA-responsive lateral rooting (Fig. 3*C*) in the weak *pex6-2* allele or the strong *pex6-4* allele.

We also examined the impact of combining *pex1-1* with *pex26-1* (37), which is defective in the tether that recruits the PEX1–PEX6 hexamer to the peroxisome (17). In contrast to the restorative or neutral effects on *pex6* mutants, we found detrimental effects when combining *pex1-1* with *pex26-1* (Fig. 3). The *pex1-1 pex26-1* double mutant scarcely grew in the absence of sucrose

(Fig. 3*A*) and remained fully resistant to IBA (Fig. 3 *A* and *C*) and 2,4-DB (Fig. 3*B*), demonstrating that the *pex1-1* mutation was not beneficial to all peroxisomal ATPase complex mutants.

Monitoring overall growth of the suite of single and double mutants revealed that *pex1-1* resembled WT throughout development (Fig. 4). As previously documented (37), *pex6-2* displayed minimal growth defects, whereas *pex6-1*, *pex6-3*, *pex6-4*, and *pex26-1* seedlings were small and pale (Fig. 4 *A* and *B*). We found that *pex1-1* generally increased root growth (Fig. 4 *A* and *B*) and rosette size (Fig. 4*B*) of *pex6* seedlings. Unlike the worsened seedling growth without sucrose (Fig. 3*A*), *pex1-1* did not notably alter *pex26-1* growth when sucrose-supplemented (Fig. 4 *A* and *B*) or following transfer to soil (Fig. 4*C*). Whereas mature *pex6-2*, *pex6-4*, and *pex26-1* plants resembled WT with or without *pex1-1*, the *pex1-1*mutation appeared to alleviate the smaller adult plant size of *pex6-1* and *pex6-3* mutants (Fig. 4*C*).

To examine the molecular consequences of the *pex1-1* lesion, we compared PTS2 processing in seedlings. As with *pex6-1*, *pex1-1* slightly improved PTS2 processing of PMDH in *pex6-3* (Fig. 3*D*). In contrast, *pex1-1* did not notably alter PTS2 processing in *pex6-2* or *pex6-4* (Fig. 3*D*), and PTS2 processing of thiolase and PMDH in *pex26-1* was worsened by *pex1-1* (Fig. 3*D*). Thus, the effects of *pex1-1* on PTS2 processing mirrored the suppression seen in β-oxidation phenotypes.

We also monitored levels of several peroxisomal matrix proteins in the double mutants. Catalase levels are elevated in certain peroxisome-defective mutants (56), perhaps because catalase undergoes less oxidative damage and degradation when β-oxidation is impaired. Consistent with the changes in β-oxidation phenotypes (Fig. 3 *A*–*C*), *pex1-1* lessened catalase accumulation in the *pex6-3* mutant and further elevated catalase levels in *pex26-1* (Fig. 3*D*). *pex1-1* did not dramatically alter catalase levels in *pex6-1*, *pex6-2*,

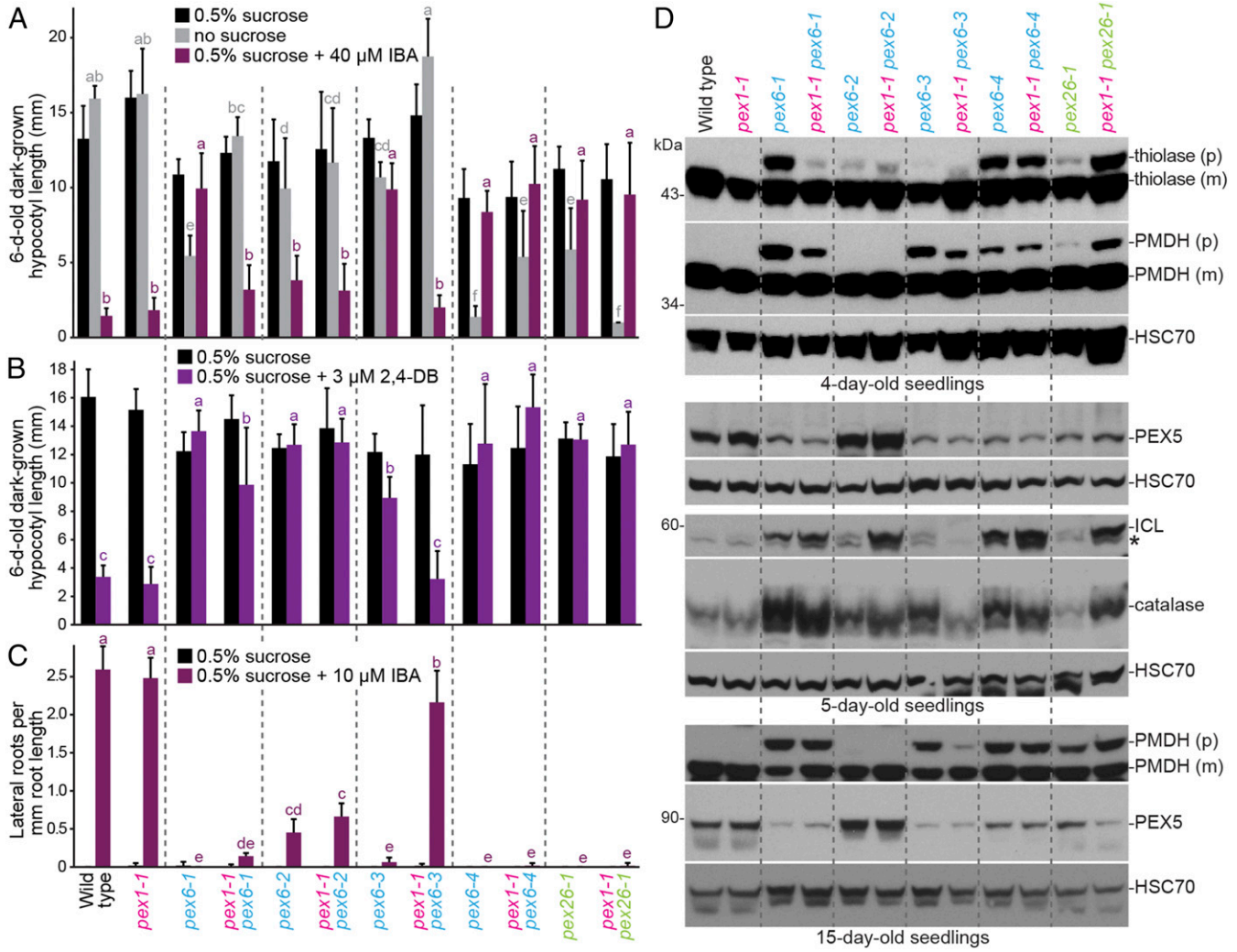

Fig. 3. *pex1-1* ameliorates *pex6-1* and *pex6-3* and worsens *pex26-1* defects without restoring PEX5 levels. (*A*) *pex1-1* increases the sensitivity of dark-grown *pex6-1* and *pex6-3* seedlings to the inhibitory effects of IBA and reduces dependence on exogenous sucrose for hypocotyl elongation but increases *pex26-1* sucrose dependence. Seedlings were grown as in the legend to Fig. 1*C*. Bars indicate mean hypocotyl lengths ($n \geq 13$), and error bars indicate SD. (*B*) *pex1-1* increases sensitivity of dark-grown *pex6-1* and *pex6-3* seedlings to the inhibitory effects of 2,4-DB on hypocotyl elongation. Seedlings were grown as in the legend to Fig. 1*C*. Bars indicate mean hypocotyl lengths ($n \geq 12$), and error bars indicate SD. (*C*) *pex1-1* increases sensitivity of light-grown *pex6-3* seedlings to the stimulatory effects of IBA on lateral root production. Seedlings were grown on control medium for 4 d followed by 4 d on medium with or without 10 μM IBA under constant yellow-filtered light. Bars indicate mean lateral root densities ($n \geq 8$), and error bars indicate SD. In *A*–*C*, means not sharing a letter above the bar are significantly different as determined by one-way ANOVA ($P < 0.001$). (*D*) *pex1-1* differentially impacts PTS2 processing and peroxisomal protein levels in *pex6* and *pex26-1* seedlings. Immunoblots of 4- (*Top*), 5- (*Middle*), and 15-d-old (*Bottom*) light-grown seedling extracts were serially probed with antibodies to the indicated proteins. The positions of molecular mass markers (in kilodaltons) are indicated on the left. For thiolase and PMDH, precursor (p) and mature (m) proteins are indicated. HSC70 is a loading control. An asterisk indicates a cross-reacting band in the ICL panels.

or *pex6-4* (Fig. 3*D*), adding to the evidence that *pex1-1* does not uniformly restore all *pex6* mutants' defects.

The glyoxylate cycle enzyme isocitrate lyase (ICL) is degraded during early seedling development (57) as the glyoxylate cycle becomes obsolete, and *pex6* mutants degrade ICL more slowly than WT (44, 57). We found that changes in ICL levels in 5-d-old seedlings mirrored catalase changes; *pex1-1* decreased ICL levels in *pex6-3* and further increased ICL levels in *pex26-1* but did not decrease ICL levels in *pex6-1*, *pex6-2*, or *pex6-4* (Fig. 3*D*).

***pex1-1* Improves Oil Body Utilization in *pex6-1* and *pex6-3*.** Because *pex6* and *pex26* mutants inefficiently utilize cotyledon oil bodies (37), we examined oil bodies by staining neutral lipids with Nile red. Confocal microscopy revealed persisting oil bodies in 5-d-old *pex6-1*, *pex6-3*, *pex6-4*, and *pex26-1* pavement and hypocotyl cells that were not observed in WT or *pex1-1* (Fig. 5). *pex1-1* alleviated oil body persistence in *pex6-1* and *pex6-3* and partially reduced oil body persistence in *pex6-4*, but failed to alleviate oil body persistence in *pex26-1* (Fig. 5). The improvement of oil body utilization conferred by *pex1-1* mirrored and presumably explains the improved growth of these lines without supplemental sucrose (Fig. 3*A*).

***pex1-1* Slightly Improves GFP-PTS1 Import in *pex6-1* and *pex6-3*.** The minor improvement of PTS2 processing observed when *pex1-1* was combined with *pex6-1* or *pex6-3* (Fig. 3*D*) suggested that *pex1-1* might be improving matrix protein import. To directly assess import, we examined the localization of GFP-PTS1 in the *pex1-1* double mutants by using confocal microscopy. WT, *pex1-1*, *pex6-2*, and *pex1-1 pex6-2* displayed similar GFP-PTS1 puncta, and GFP-PTS1 remained largely cytosolic in the *pex1-1 pex6-4* double mutant (Fig. 5). In contrast, the predominantly cytosolic GFP-PTS1 in *pex6-1* and *pex6-3* mutants was slightly improved by *pex1-1*, as evidenced by the appearance of some GFP-PTS1 puncta in the *pex1-1 pex6-1* and *pex1-1 pex6-3* double mutants (Fig. 5).

***pex1-1* Does Not Restore PEX5 Levels in *pex6* Mutants.** Most *Arabidopsis* *pex6* mutants (35, 37) and human *pex6* patients (36) have low PEX5 levels, presumably because PEX5 is polyubiquitinated and degraded in the absence of efficient recycling. In contrast, immunoblotting revealed that PEX5 levels were not decreased in *pex1-1* (Figs. 2*B* and 3*D*). Surprisingly, PEX5 levels remained low in seedlings when *pex1-1* was combined with *pex6-1, pex6-3*, *pex6-4*, or *pex26-1* (Fig. 3*D*). Moreover, PEX5 levels remained elevated when *pex1-1* was combined with *pex6-2* (Fig. 3*D*). As expected, PEX5 levels remained low in *pex1-1 pex6-1 35S:HA-PEX1* (Fig. 2*B*).

Because *pex1-1* did not restore PEX5 levels in *pex6* mutants, we interrogated PEX5 localization by using centrifugation to separate cytosolic and membrane-associated proteins. PEX5 is excessively membrane associated in *pex6-1* (46) and *pex6-3* (37). We found that PEX5 distribution between the supernatant and pellet in *pex1-1* resembled WT and that *pex1-1* did not dramatically alter the excessive association of PEX5 with the membrane fraction in *pex6-1* (Fig. 6) or *pex6-3* (Fig. S3).

We also examined PEX1 and PEX6 localization in these fractionation experiments. Like PEX5, PEX1 and PEX6 were approximately evenly distributed between the supernatant and pellet fractions in WT (Fig. 6 and Fig. S3). This distribution did not markedly change in the *pex1-1* or *pex6* single or double mutants (Fig. 6 and Fig. S3), suggesting that the *pex6-1* and *pex6-3* mutations do not impair peroxisome association of the pex6 protein and that altering pex6 localization is not the basis of *pex1-1* suppression.

Overexpressing *PEX5* in *pex1-1 pex6-1* Further Rescues *pex6-1* Deficiencies. Because PEX5 levels remained low in *pex1-1 pex6-1* (Fig. 3*D*), we tested whether overexpressing *PEX5* could further restore peroxisome function. We found no discernible effect of excess PEX5 on *pex1-1* or WT growth, IBA sensitivity, or PTS2 processing (Fig. 7). As previously reported (35, 44), excess PEX5 improved *pex6-1* growth without sucrose (Fig. 7*A*) and partially restored PTS2 processing (Fig. 7*C*). We found that overexpressing *PEX5* in *pex1-1 pex6-1* further improved growth without sucrose (Fig. 7*A*) and IBA responsiveness (Fig. 7 *A* and *B*), although a slight defect in PTS2 processing remained (Fig. 7*C*). This additive *pex6-1* suppression by *pex1-1* and *35S:PEX5* suggests that *pex1-1 pex6-1* remains limited by decreased PEX5 recycling.

Preventing Autophagy Also Restores Peroxisome Function in *pex6-1*. To illuminate the mechanism of *pex6-1* suppression, we compared the suppression effects of *pex1-1* vs. a previously characterized *pex6* suppressor, *pex13-1*, a partial loss-of-function allele that may ameliorate *pex6-1* defects by decreasing PEX5 docking at the

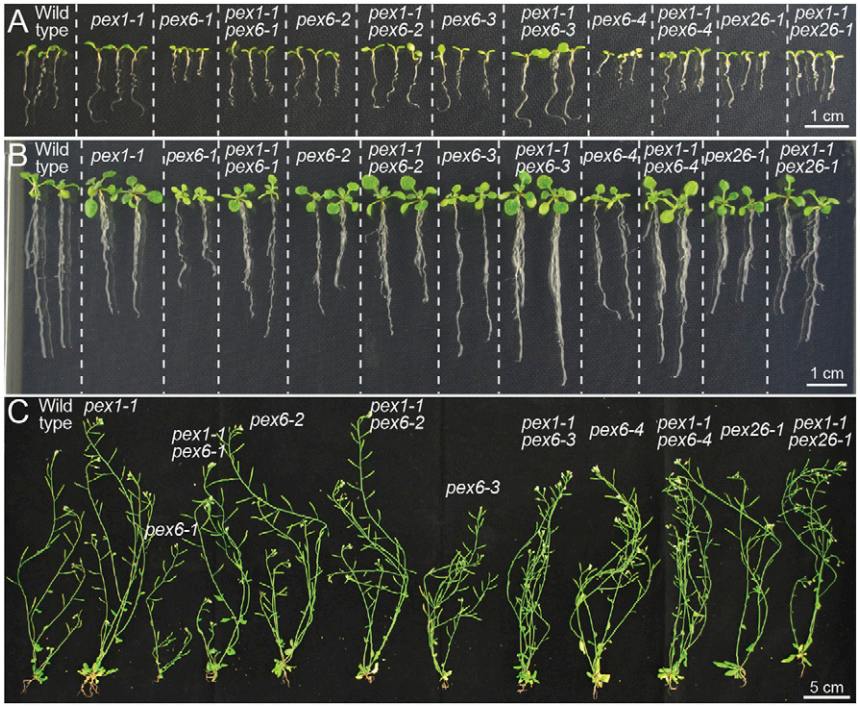

Fig. 4. *pex1-1* lessens *pex6* growth defects. (*A* and *B*) *pex1-1* resembles WT and restores *pex6* mutant defects in size and pigmentation. Seedlings at 7 d old (*A*) and 14 d old (*B*) were grown on sucrose-containing medium before photography (Scale bar: 1 cm.) (*C*) *pex1-1* resembles WT and rescues *pex6-1* and *pex6-3* defects in adult size. Plants were transferred to soil after 14 d on sucrose-containing medium and photographed after an additional 4 wk in light. (Scale bar: 5 cm.)

CELL BIOLOGY

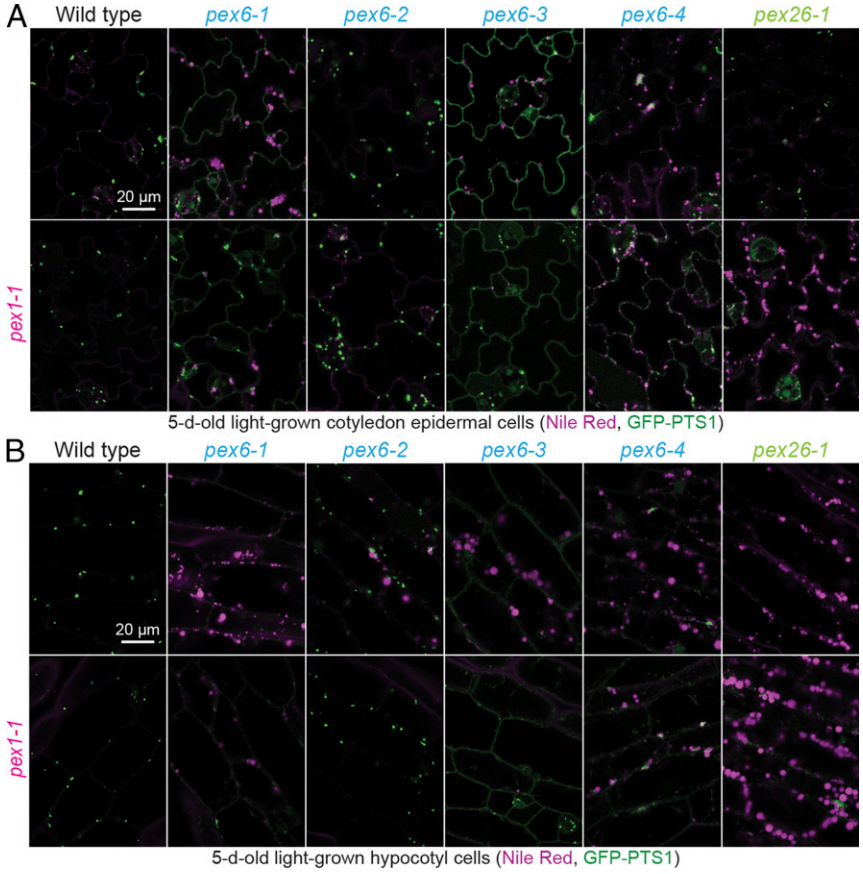

Fig. 5. *pex1-1* slightly improves *pex6-1* and *pex6-3* GFP-PTS1 import and improves oil body utilization in *pex6* mutants but does not improve oil body utilization in *pex26-1*. Confocal images of cotyledon epidermal cells (*A*) and hypocotyl cells (*B*) of 5-d-old seedlings carrying *35S:GFP-PTS1* (green) stained with Nile red (magenta). Emissions were collected at 490–519 nm for GFP and 587–643 nm for Nile red. Seedlings were screened for germination 2 d after plating, and individuals that had germinated by day 2 were imaged on day 5. (Scale bar: 20 μm.)

peroxisome (46). We found that *pex1-1* was more effective than *pex13-1* in restoring growth without sucrose, IBA responsiveness, and PTS2 processing to *pex6-1* (Fig. 8 *A* and *B*). The *pex1-1 pex6-1 pex13-1* triple mutant resembled the *pex1-1 pex6-1* double mutant in these assays (Fig. 8 *A* and *B*), indicating that decreasing PEX13 levels did not provide additional benefit to *pex1-1 pex6-1*.

Autophagy is a process by which eukaryotes degrade organelles (reviewed in ref. 58), including peroxisomes (reviewed in ref. 59). Because preventing autophagy ameliorates some *pex1-3* defects (38), we examined the contributions of autophagy to *pex6-1* phenotypes by crossing to the *atg7-3*–null allele (60, 61). *atg7-3* improved *pex6-1* growth without sucrose, IBA responsiveness, and PTS2 processing, although not as markedly as *pex1-1* (Fig. 8 *A* and *B*). Introducing *pex1-1* to *pex6-1 atg7-3* further improved PTS2 processing (Fig. 8*B*). PEX5 levels remained low in the *pex1-1 pex6-1 atg7-3* and *pex1-1 pex6-1 pex13-1* triple mutants (Fig. 8*B*), indicating that the physiological rescue (Fig. 8*A*) was accomplished without restoring PEX5 levels. We also examined PEX1 and PEX6 levels in these mutants and found that both peroxins were elevated in all genotypes that included the *atg7-3* mutation, suggesting that PEX1 and PEX6 levels can be modulated by autophagy.

Because *atg7-3* improved PTS2 processing in *pex6-1*, we also monitored GFP-PTS1 localization and oil body persistence in these mutants. Like WT, 5-d-old *atg7-3* seedlings lacked oil bodies and displayed GFP-PTS1 puncta (Fig. 8*C*). Consistent with the restoration of growth without sucrose (Fig. 8*A*), *atg7-3* restored oil body utilization in *pex6-1* (Fig. 8*C*). However, GFP-PTS1 remained largely cytosolic in *pex6-1 atg7-3* (Fig. 8*C*). In contrast, GFP-PTS1 appeared largely punctate in the *pex1-1 pex6-1 atg7-3* triple mutant (Fig. 8*C*), indicating that *pex1-1* and *atg7-3* synergistically improved *pex6-1* matrix protein import without increasing PTS1 receptor levels.

Discussion

The peroxins in the ATPase complex (PEX1, PEX6, and PEX26) are implicated in removing PEX5 from the peroxisomal membrane after cargo delivery (14), allowing recycled PEX5 to promote another round of matrix protein import. Analyses of *Arabidopsis pex1* (38), *pex6* (35, 37, 44), and *pex26* (17, 37) loss-of-function mutants have begun to elucidate the roles of the ATPase complex peroxins in PEX5 management (reviewed in ref. 3). For example, four *Arabidopsis pex6* missense mutations confer disparate phenotypes that suggest impairment of different aspects of PEX6 function (35, 37, 44). In an effort to expand our understanding of PEX6, we conducted a screen for *pex6-1* suppressors and characterized the *pex1-1* missense allele that emerged from this screen (Fig. 1).

Because PEX1 and PEX6 are present in a 1:1 ratio in a heterohexamer, the *pex1-1* semidominant suppression (Fig. 1*C*) likely reflects the multiple possible combinations of pex1-1 and PEX1 with pex6-1. For example, only 12.5% of heterohexamers would be expected to carry three WT PEX1 subunits in a *PEX1*/*pex1-1* heterozygote. Indeed, the *Arabidopsis pex1-3* missense allele confers peroxisome-related defects when heterozygous and lethality when homozygous (38), highlighting the sensitivity of this hexamer to perturbation even when some WT PEX1 remains.

***pex1-1* Ameliorates Defects in a Subset of *pex6* Alleles Without Restoring PEX5 Levels.** *pex1-1* did not similarly rescue all *pex6* mutants (Table S1). *pex1-1* had little or negative effects on *pex6-2* physiological and molecular defects (Fig. 3). *pex1-1* slightly improved *pex6-4* oil body utilization (Fig. 5) and growth in the absence of sucrose (Fig. 3*A*) without notably improving IBA responsiveness or PTS2 processing (Fig. 3 *A*, *C*, and *D*). In contrast, *pex1-1* improved *pex6-1* and *pex6-3* IBA responsiveness (Fig. 3 *A* and *C*), growth on medium lacking sucrose (Fig. 3*A*), PTS2 processing (Fig. 3*D*), GFP-PTS1 import (Fig. 5), and oil body utilization (Fig. 5). Interestingly, *pex1-1* improved *pex6-3* more fully than the *pex6-1* allele used in our

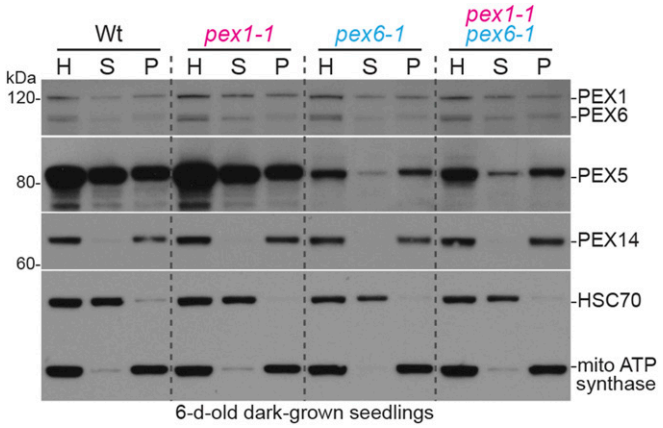

Fig. 6. PEX5 remains excessively membrane-associated in *pex1-1 pex6-1*. Homogenates (H) prepared from 6-d-old dark-grown WT, *pex1-1*, *pex6-1*, and *pex1-1 pex6-1* seedlings were separated by centrifugation to isolate cytosolic supernatant (S) and an organellar pellet, which was resuspended and recentrifuged to provide a final organellar pellet (P) fraction. Fractions were subjected to immunoblotting with the indicated antibodies. HSC70 is cytosolic, and mitochondrial (mito) ATP synthase subunit α and PEX14 localize in the organelle fraction. The positions of molecular mass markers (in kilodaltons) are indicated on the left.

original screen (Fig. 3). As implied by the linear model shown in Fig. 1*B*, examination of analogous residues in the crystal structure of the related human p97 protein (62, 63) reveals that *pex1-1* alters a residue adjacent to the AAA1 domain (Fig. S1), which is separated by a linker from the AAA2 domain where the lesions in *pex6-1*, *pex6-3*, and *pex6-4* mutants are found (37). The pex1-1 analogous residue in human p97 (Gly376) is at least 25 Å from the residues corresponding to the pex6-1, pex6-3, and pex6-4 mutations in the neighboring subunit (Fig. S1), indicating that suppression is unlikely to arise from direct interaction of the mutated residues. In contrast, the analogous pex1-1 residue is only ∼7 Å from the ATP bound by the AAA1 domain and ∼11 Å from the linker that connects the AAA1 and AAA2 domains, hinting that pex1-1 might influence AAA1 ATP binding and/or communication between the AAA1 and AAA2 domains (Fig. S1).

Adding to the evidence of *pex1-1* rescue specificity is the observation that the other two reported *PEX1* missense alleles, the mild *pex1-2* allele and the more severe *pex1-3* allele, confer lethality in combination with *pex6-1* (38), suggesting that simply decreasing PEX1 function does not improve activity of complexes carrying mutated PEX6. Moreover, *pex1-1* worsened rather than improved *pex26-1* growth defects (Fig. 3*A*), PTS2 processing (Fig. 3*D*), catalase and ICL levels (Fig. 3*D*), and oil body utilization (Fig. 5). This exacerbation suggests that pex1-1 further impedes ATPase function in *pex26-1* even though *pex1-1* does not notably impair peroxisome function as a single mutant.

Interestingly, the pattern of *pex1-1* suppression of *pex6* and *pex26* alleles mirrored the range of restorative or exacerbative effects of overexpressing *PEX5* in these mutants. *PEX5* overexpression worsens the peroxisome-related defects of *pex26-1* (37), fails to rescue *pex6-2* (44), slightly rescues a subset of *pex6-4* defects (37), substantially rescues *pex6-1* (35, 37), and most fully rescues *pex6-3* (37). PEX5 accumulation in the peroxisomal membrane is detrimental to peroxisome function (46, 64), and the parallel suppression patterns conferred by *PEX5* overexpression or *pex1-1* reinforces the hypothesis that these *pex6* and *pex26-1* mutations differentially disrupt retrotranslocation of monoubiquitinated PEX5 for recycling vs. retrotranslocation of polyubiquitinated PEX5 for proteasomal degradation (37). Analysis of PEX5 ubiquitination states in these mutants would be useful to test this hypothesis.

We initially expected that *pex1-1* improvement of *pex6* physiology and matrix protein import might be caused by improved PEX5 recycling. The *pex6-1*, *pex6-3*, *pex6-4*, and *pex26-1* mutants have low PEX5 levels (35, 37) that can be increased by proteasomal inhibition (37, 52), suggesting that PEX5 is ubiquitinated and degraded when the ATPase complex is dysfunctional. Contrary to our expectations, PEX5 levels remained low in all *pex1-1* combinations with *pex6* and *pex26* mutant except *pex6-2* (Fig. 3*D*), which has elevated rather than reduced PEX5 levels (37). Moreover, examination of PEX5 membrane association to determine whether *pex1-1* might improve removal of PEX5 from the membrane without decreasing PEX5 degradation revealed that PEX5 remained excessively membrane-associated in *pex1-1 pex6-1* and *pex1-1 pex6-3* (Fig. 6 and Fig. S3). Although a slight recycling improvement would be difficult to discern in this assay, these results hint that dysregulation of PEX6 functions in addition to PEX5 retrotranslocation may contribute to *pex6* phenotypes, as has been suggested in plants (44, 57) and yeast (65). These hypothetical ubiquitinated PEX1–PEX6 clients might be generated by the PEX2–PEX10–PEX12 complex (66) or other peroxisome-associated ubiquitin–protein ligases (67).

Diverse *pex6-1* Suppression Mechanisms Suggest Complexity of PEX6 Functions. Decreasing *PEX13* expression via the *pex13-1* allele partially suppresses *pex6-1* physiological defects without notably improving PTS2 processing or PEX5 levels (Fig. 8 *A* and *B*) (46). These findings suggest that *pex6-1* defects stem not only from reduced matrix protein import but also from excessive PEX5 buildup

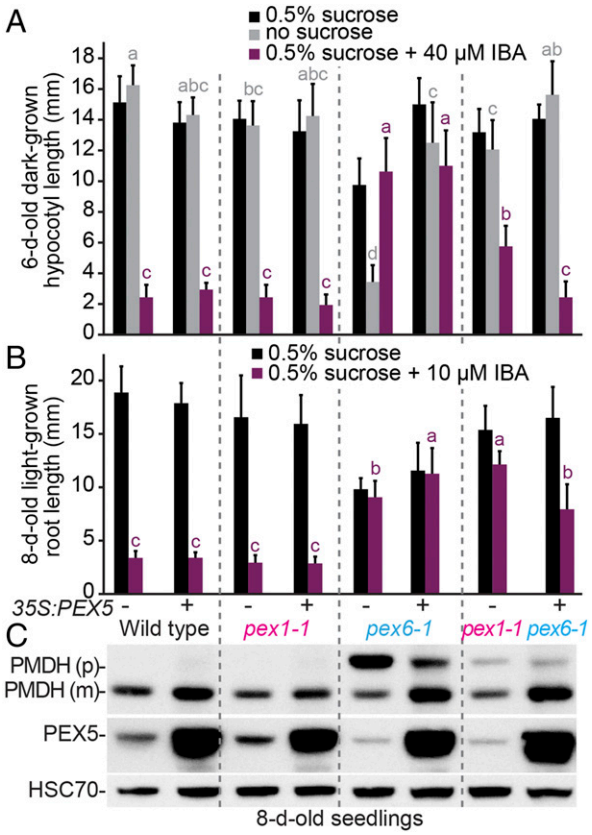

Fig. 7. *pex1-1* and overexpressing *PEX5* additively restore *pex6-1* defects. (*A* and *B*) Overexpressing *PEX5* improves *pex1-1 pex6-1* dark-grown (*A*) and light-grown (*B*) physiology. Plant lines with (+) and without (–) *35S:PEX5* were grown on the indicated media for 1 d under yellow-filtered light before moving to darkness for 5 d (*A*) or were grown for 8 d under continuous yellow-filtered light (*B*). Bars indicate mean hypocotyl lengths (*A*; $n \geq 14$) or root lengths (*B*; $n \geq 13$), and error bars indicate SD. Means not sharing a letter above the bar are significantly different as determined by one-way ANOVA ($P < 0.001$). (*C*) Overexpressing *PEX5* improves PTS2 processing in *pex1-1 pex6-1* seedlings. An immunoblot of 8-d-old light-grown seedling extracts was serially probed with antibodies to the indicated proteins. Precursor (p) and mature (m) PMDH are indicated. HSC70 is a loading control.

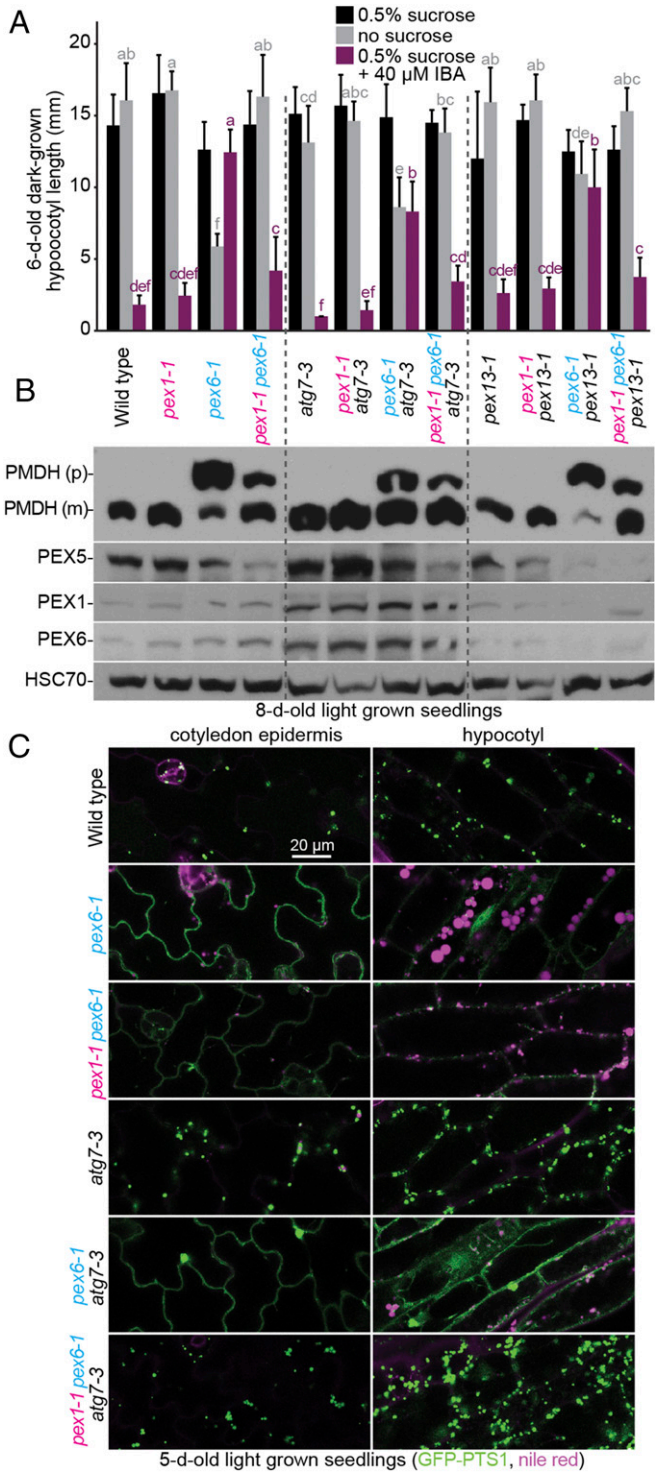

Fig. 8. *pex1-1* augments benefits provided to *pex6-1* by preventing autophagy without increasing PEX5 levels. (*A*) *pex1-1*, *atg7-3*, and *pex13-1* improve *pex6-1* IBA responsiveness and growth without sucrose, and *pex1-1* further increases *atg7-3* benefits. Seedlings were grown as in the legend to Fig. 1C. Bars indicate mean hypocotyl lengths (n = 16), and error bars indicate SD. Means not sharing a letter above the bar are significantly different as determined by one-way ANOVA ($P < 0.001$). (*B*) Preventing autophagy increases PTS2 processing in *pex6-1*, and this increase is further improved by *pex1-1*. An immunoblot of 8-d-old light-grown seedling extracts was serially probed with antibodies to the indicated proteins. Precursor (p) and mature (m) PMDH are indicated. HSC70 is a loading control. (*C*) Preventing autophagy and *pex1-1* synergistically improve GFP-PTS1 import in *pex6-1*. Confocal images of cotyledon epidermal and hypocotyl cells were collected after staining 5-d-old seedlings carrying *35S:GFP-PTS1* (green) with Nile red (magenta). Emissions were collected at 490–526 nm for GFP and 586–643 nm for Nile red.

in the membrane and that *pex13-1* relieves this detrimental accumulation by decreasing PEX5 peroxisomal docking. Our observation that *pex1-1* slightly improves *pex6-1* and *pex6-3* PTS2 processing (Fig. 3*D*) and matrix protein import (Fig. 5*A*) implies that *pex1-1* does not act by reducing PEX5 docking at the peroxisome.

We found that the autophagy-defective *atg7-3*–null allele also partially ameliorated physiological and molecular defects of *pex6-1* (Fig. 8), suggesting that decreasing constitutive pexophagy is beneficial or that *pex6-1* suffers from heightened pexophagy. Similarly, preventing autophagy lessens the physiological defects of yeast *pex1* and *pex6* mutants (65), mammalian *PEX1* and *PEX26* knockdown cells (20), and the *Arabidopsis PEX1*/*pex1-3* heterozygote (38). This suppression implies that, when the retrotranslocation machinery is disabled, polyubiquitinated PEX5 (or other ATPase clients) marooned on the peroxisome membrane triggers not only proteasomal degradation of PEX5 (37, 52), but also pexophagy of the entire organelle. Alternatively or in addition, the elevated PEX1–PEX6 levels that accompany autophagy prevention (Fig. 8*B*) could provide additional ATPase function that slightly improves peroxisome function.

Preventing autophagy also improves peroxisome function in the *Arabidopsis lon2* mutant. LON2 is a peroxisomal protease that promotes sustained matrix protein import (68) by preventing premature autophagy of peroxisomes (69). Unlike the apparently complete suppression of multiple *lon2-2* phenotypes when autophagy is precluded (69, 70), preventing autophagy by introducing *atg7-3* only slightly ameliorated *pex6-1* (Fig. 8) or *PEX1*/*pex1-3* (38) defects, confirming that the PEX1–PEX6 hexamer contributes to peroxisome functions beyond the prevention of pexophagy.

Because PEX5 levels remained low in *pex1-1 pex6-1* (Fig. 3*D*), we hypothesized that *pex1-1* might increase removal and proteasomal degradation of polyubiquitinated PEX5 in the peroxisome membrane, thus reducing PEX5-triggered pexophagy and increasing *pex6-1* peroxisome function without restoring PEX5 levels. However, we found that combining *pex1-1* with *pex6-1 atg7-3* further improved peroxisome function; matrix protein import resembled WT in *pex1-1 pex6-1 atg7-3* (Fig. 8*C*) despite low PEX5 levels (Fig. 8*B*). The observation that *pex1-1* further improved *pex6-1* import even in the complete absence of autophagy (Fig. 8*C*) indicates that *pex1-1* does not primarily suppress *pex6-1* by preventing pexophagy. Because preventing autophagy in *pex6-1* was insufficient to restore import, it follows that pex1-1 partially increases pex6-1 function. Perhaps preventing autophagy allows more time for the pex1-1 pex6-1 hexamer to extract PEX5 (for recycling or degradation), resulting in improved peroxisome import and function.

In addition to decreased PEX5 levels (35), PEX5 is excessively membrane-associated in *pex6-1* (46); neither defect was relieved by *pex1-1* (Figs. 3*D* and 6). Moreover, increasing PEX5 levels via transgenics (35) or by combination with a ubiquitination machinery mutant (71) partially suppresses *pex6-1* defects. Overexpressing *PEX5* further ameliorated defects remaining in the *pex1-1 pex6-1* double mutant (Fig. 7). This additive rescue suggests that *pex1-1* and *PEX5* overexpression may restore different facets of *pex6* dysfunction.

Our observations that *pex6* symptoms can be relieved through multiple avenues (Table S1) without restoring PEX5 recycling, the sole known function of PEX6, suggest that PEX1–PEX6 has additional functions. For example, our results suggest that PEX1–PEX6 removes a pexophagy-promoting signal from the peroxisome membrane. Moreover, several *Arabidopsis pex6* mutants retain seedling oil bodies after they have been fully utilized in WT seedlings (37). Similarly, mice lacking PEX5 accumulate lipid droplets in liver cells (45). Regulation of TAG mobilization is complex; overexpressing *PEX5* (37), preventing autophagy (Fig. 8*C*), or introducing *pex1-1* (Figs. 5 and 8*C*) each restore oil body utilization in *Arabidopsis pex6-1*. Our characterization of

this *pex1* allele that selectively restores a subset of *pex6* mutant defects expands our understanding of the peroxisomal ATPase complex and provides tools for the future investigation of the roles of this essential ATPase complex in recycling PEX5, preventing pexophagy, and promoting oil body utilization.

Materials and Methods

Plant Materials and Growth Conditions. The Columbia-0 (Col-0) accession of *Arabidopsis thaliana* was the WT control, and all mutants were in the Col-0 background. *atg7-3* (SAIL_11_H07; 60, 61), *pex6-1* (35), *pex6-2* (44), *pex6-3* (37), *pex6-4* (37), *pex13-1* (SALK_006744; 46), *pex13-1 pex6-1* (46), *pex26-1* (37), and *pxa1-1* (55) were previously described. *pex1-1* and *pex1-1 pex6-1* mutants were backcrossed at least once before phenotypic assays. Genotypes were determined by using PCR-based markers (Table S2). Seedlings were moved from plates to soil (SunGro MetroMix 366) after 1–2 wk and were grown under constant white light at 22 °C.

We crossed previously described WT *35S:PEX5* and *pex6-1 35S:PEX5* expressing a *PEX5* cDNA (35) to *pex1-1 pex6-1* to isolate *pex1-1* and *pex1-1 pex6-1* lines overexpressing *PEX5*, respectively. Transgenic plants were selected by using Basta resistance and by PCR-amplifying *PEX5* using intron-spanning primers (Table S2).

To isolate peroxisome-targeted GFP in *pex1-1* and double/triple mutants, we crossed *pex1-1* to WT, *pex6-2*, *pex6-3*, *pex6-4*, or *pex26-1* containing *35S:GFP-PTS1* (35, 37, 44), crossed *pex1-1 pex6-1* to *pex6-1 35S:GFP-PTS1* (35), and crossed *pex1-1 pex6-1 35S:GFP-PTS1* to *atg7-3 35S:GFP-PTS1*. The transgene was tracked by using PCR amplification with primers annealing to the promoter and *GFP* (Table S2).

Seedlings were grown on plant nutrient (PN) medium (72) solidified with 0.6% (wt/vol) agar and supplemented with 0.5% (wt/vol) sucrose (PNS medium) and IBA from an ethanol-dissolved stock solution as indicated. Physiological assays monitoring seedling growth and IBA responsiveness were conducted as described previously (37) and were repeated at least twice with similar results.

Mutant Isolation. *pex6-1* seeds were soaked in 0.12% EMS for 16 h in the dark, washed extensively, and allowed to germinate in liquid 1/6× PN medium supplemented with 0.5% sucrose to promote germination. Seedlings were transferred to soil to allow M_2 seed set. *pex1-1* was isolated by screening *pex6-1* M_2 seedlings grown on PN for individuals with elongated dark-grown hypocotyls. Putative suppressors were transferred to PNS in the light to recover before transferring to soil, and progeny were retested for the ability to elongate hypocotyls in the dark without sucrose.

Whole-Genome Sequencing. Approximately 2,000 backcrossed seedlings were grown under continuous white light for 14 d on sterile filter paper on PNS. Seedlings from three lines were pooled to reduce the appearance of homozygous noncausal background mutations, and genomic DNA was prepared as described previously (73). DNA was sequenced at the Genome Technology Access Center at Washington University in St. Louis by using an Illumina HiSEq 2000 sequencer and was analyzed as described previously (69, 74) to identify EMS-consistent lesions in predicted coding sequences, introns, and UTRs that were absent in our laboratory version of Col-0. More than 80% of the genome had 10-fold sequence coverage.

DNA Constructs and Plant Transformation. *35S:HA-PEX6* was previously described (37). A *PEX1* cDNA in pENTR/SD-DTOPO was transferred into the pEG201 destination vector (75) using LR clonase II (Invitrogen) to give *35S:HA-PEX1*, which was transformed into *Agrobacterium tumefaciens* GV3101 (pMP90) (76) and used to transform *pex1-1 pex6-1* and WT using the floral dip method (77). Transformants were selected on PNS plates containing 8–10 μg/mL Basta; homozygous lines were identified by monitoring Basta resistance in the T_3 generation.

Immunoblot Analysis. Seedling tissue was prepared for immunoblotting as described previously (37). Primary antibodies were incubated with membranes overnight as follows: rabbit anti-PEX1 (1:200; ref. 38), anti-PEX5 (1:100; ref. 35), anti-PEX6 (1:800–1,000; ref. 46), anti-PEX14 (1:10,000; Agrisera AS08), anti-catalase (1:20,000; ref. 78), anti-ICL (1:1,000; ref. 79), anti-PMDH2 (1:2,000; ref. 80), anti-thiolase (1:2,500–1:5,000; ref. 57), mouse anti-mitochondrial ATP synthase subunit α (1:2,000; MitoScience MS507) and anti-HSC70 (1:50,000–1:100,000; SPA-817; StressGen Biotechnologies), and rat anti-HA (1:100–1:500; clone 3F10; Roche). Membranes were incubated for 3–6 h with HRP-conjugated secondary antibodies (1:5,000) before washing and imaging using WesternBright ECL substrate (Advansta). Membranes were sequentially probed with various antibodies without stripping. Films were scanned by using a flatbed scanner. Immunoblotting experiments were performed at least twice with similar results.

Confocal Fluorescence Microscopy. Seedlings were grown under continuous light on PNS, and germination was scored 2 or 3 d after plating. Cotyledons and hypocotyls from individuals with emerged radicles at germination scoring were stained with 5 μg/mL Nile red and imaged on day 5. A Carl Zeiss 710 confocal microscope with a 63× oil-immersion objective and a Meta detector was used to capture fluorescence. A 488-nm Argon laser was used to image 0.8-μm optical sections. Each image is an average of four images with 12-bit depth. Confocal microscopy experiments were repeated at least four times with similar results.

Cell Fractionation. An approximately equal mass (±0.03 g) of seedlings was collected from each genotype. Tissue was processed as described previously (64). Fractionation experiments were repeated twice with similar results.

Statistical Analysis. One-way ANOVA with Duncan's test was used to assess statistical significance (SPSS Statistics, version 24; IBM). Different letters above bars in the figures denote significant differences ($P < 0.001$).

Accession Numbers. Sequence data can be found in the *Arabidopsis* Genome Initiative under the accession numbers *At5g08470* (*PEX1*) and *At1g03000* (*PEX6*). Other proteins aligned in Fig. 1*B* were human PEX1 (NP_000457), PEX6 (NP_000278.3), and p97 (NP_009057).

ACKNOWLEDGMENTS. We thank Shino Goto and Mikio Nishimura for the *PEX1* cDNA; Masayoshi Maeshima, Steven Smith, and Richard Trelease antibodies recognizing ICL, PMDH, and catalase, respectively; and Yun-Ting Kao, Kathryn Smith, and Zachary Wright for critical comments on the manuscript. This research was supported by National Institutes of Health (NIH) Grant R01GM079177, National Science Foundation (NSF) Grant MCB-1516966, Robert A. Welch Foundation Grant C-1309, NSF Graduate Research Fellowship DGE-0940902 (to K.L.G.), and an NSF training program EHR-0966303 (to K.L.G.). Genomic sequencing at the Genome Technology Access Center at Washington University School of Medicine was supported by NIH Grants P30CA91842 and UL1RR024992. Confocal microscopy performed in this study used equipment obtained through NIH Shared Instrumentation Grant S10RR026399.

1. Nyathi Y, et al. (2010) The *Arabidopsis* peroxisomal ABC transporter, comatose, complements the *Saccharomyces cerevisiae pxa1 pxa2*Δ mutant for metabolism of long-chain fatty acids and exhibits fatty acyl-CoA-stimulated ATPase activity. *J Biol Chem* 285:29892–29902.
2. Bartel B, Burkhart SE, Fleming WA (2014) Protein transport in and out of plant peroxisomes. *Molecular Machines Involved in Peroxisome Biogenesis and Maintenance*, eds Brocard C, Hartig A (Springer, Vienna), pp 325–345.
3. Kao YT, Gonzalez KL, Bartel B (2018) Peroxisome function, biogenesis, and dynamics in plants. *Plant Physiol* 176:162–177.
4. Hu J, et al. (2012) Plant peroxisomes: biogenesis and function. *Plant Cell* 24:2279–2303.
5. Strader LC, Bartel B (2011) Transport and metabolism of the endogenous auxin precursor indole-3-butyric acid. *Mol Plant* 4:477–486.
6. Gould SJ, Keller GA, Hosken N, Wilkinson J, Subramani S (1989) A conserved tripeptide sorts proteins to peroxisomes. *J Cell Biol* 108:1657–1664.
7. Swinkels BW, Gould SJ, Bodnar AG, Rachubinski RA, Subramani S (1991) A novel, cleavable peroxisomal targeting signal at the amino-terminus of the rat 3-ketoacyl-CoA thiolase. *EMBO J* 10:3255–3262.
8. Azevedo JE, Schliebs W (2006) Pex14p, more than just a docking protein. *Biochim Biophys Acta* 1763:1574–1584.
9. Meinecke M, et al. (2010) The peroxisomal importomer constitutes a large and highly dynamic pore. *Nat Cell Biol* 12:273–277.
10. Kerssen D, et al. (2006) Membrane association of the cycling peroxisome import receptor Pex5p. *J Biol Chem* 281:27003–27015.
11. Williams C, van den Berg M, Sprenger RR, Distel B (2007) A conserved cysteine is essential for Pex4p-dependent ubiquitination of the peroxisomal import receptor Pex5p. *J Biol Chem* 282:22534–22543.
12. Platta HW, et al. (2007) Ubiquitination of the peroxisomal import receptor Pex5p is required for its recycling. *J Cell Biol* 177:197–204.
13. Platta HW, et al. (2009) Pex2 and pex12 function as protein-ubiquitin ligases in peroxisomal protein import. *Mol Cell Biol* 29:5505–5516.
14. Platta HW, Grunau S, Rosenkranz K, Girzalsky W, Erdmann R (2005) Functional role of the AAA peroxins in dislocation of the cycling PTS1 receptor back to the cytosol. *Nat Cell Biol* 7:817–822.
15. Birschmann I, et al. (2003) Pex15p of *Saccharomyces cerevisiae* provides a molecular basis for recruitment of the AAA peroxin Pex6p to peroxisomal membranes. *Mol Biol Cell* 14:2226–2236.
16. Matsumoto N, Tamura S, Fujiki Y (2003) The pathogenic peroxin Pex26p recruits the Pex1p-Pex6p AAA ATPase complexes to peroxisomes. *Nat Cell Biol* 5:454–460.

17. Goto S, Mano S, Nakamori C, Nishimura M (2011) *Arabidopsis* ABERRANT PEROXISOME MORPHOLOGY9 is a peroxin that recruits the PEX1-PEX6 complex to peroxisomes. *Plant Cell* 23:1573–1587.
18. Platta HW, Girzalsky W, Erdmann R (2004) Ubiquitination of the peroxisomal import receptor Pex5p. *Biochem J* 384:37–45.
19. Kiel JA, Emmrich K, Meyer HE, Kunau WH (2005) Ubiquitination of the peroxisomal targeting signal type 1 receptor, Pex5p, suggests the presence of a quality control mechanism during peroxisomal matrix protein import. *J Biol Chem* 280:1921–1930.
20. Law KB, et al. (2017) The peroxisomal AAA ATPase complex prevents pexophagy and development of peroxisome biogenesis disorders. *Autophagy* 13:868–884.
21. Grimm I, Erdmann R, Girzalsky W (2016) Role of AAA(+)-proteins in peroxisome biogenesis and function. *Biochim Biophys Acta* 1863:828–837.
22. Saffian D, Grimm I, Girzalsky W, Erdmann R (2012) ATP-dependent assembly of the heteromeric Pex1p-Pex6p-complex of the peroxisomal matrix protein import machinery. *J Struct Biol* 179:126–132.
23. Gardner BM, Chowdhury S, Lander GC, Martin A (2015) The Pex1/Pex6 complex is a heterohexameric AAA+ motor with alternating and highly coordinated subunits. *J Mol Biol* 427:1375–1388.
24. Ciniawsky S, et al. (2015) Molecular snapshots of the Pex1/6 AAA+ complex in action. *Nat Commun* 6:7331.
25. Blok NB, et al. (2015) Unique double-ring structure of the peroxisomal Pex1/Pex6 ATPase complex revealed by cryo-electron microscopy. *Proc Natl Acad Sci USA* 112: E4017–E4025.
26. Gardner BM, et al. (2018) The peroxisomal AAA-ATPase Pex1/Pex6 unfolds substrates by processive threading. *Nat Commun* 9:135.
27. Saffert P, Enenkel C, Wendler P (2017) Structure and function of p97 and Pex1/6 type II AAA+ complexes. *Front Mol Biosci* 4:33.
28. Tamura S, Yasutake S, Matsumoto N, Fujiki Y (2006) Dynamic and functional assembly of the AAA peroxins, Pex1p and Pex6p, and their membrane receptor Pex26p. *J Biol Chem* 281:27693–27704.
29. Tamura S, Matsumoto N, Takeba R, Fujiki Y (2014) AAA peroxins and their recruiter Pex26p modulate the interactions of peroxins involved in peroxisomal protein import. *J Biol Chem* 289:24336–24346.
30. Seo JG, Lai CY, Miceli MV, Jazwinski SM (2007) A novel role of peroxin PEX6: suppression of aging defects in mitochondria. *Aging Cell* 6:405–413.
31. Braverman NE, et al. (2016) Peroxisome biogenesis disorders in the Zellweger spectrum: An overview of current diagnosis, clinical manifestations, and treatment guidelines. *Mol Genet Metab* 117:313–321.
32. Nito K, Kamigaki A, Kondo M, Hayashi M, Nishimura M (2007) Functional classification of *Arabidopsis* peroxisome biogenesis factors proposed from analyses of knockdown mutants. *Plant Cell Physiol* 48:763–774.
33. Kaplan CP, Thomas JE, Charlton WL, Baker A (2001) Identification and characterisation of PEX6 orthologues from plants. *Biochim Biophys Acta* 1539:173–180.
34. Lopez-Huertas E, Charlton WL, Johnson B, Graham IA, Baker A (2000) Stress induces peroxisome biogenesis genes. *EMBO J* 19:6770–6777.
35. Zolman BK, Bartel B (2004) An *Arabidopsis* indole-3-butyric acid-response mutant defective in PEROXIN6, an apparent ATPase implicated in peroxisomal function. *Proc Natl Acad Sci USA* 101:1786–1791.
36. Dodt G, Gould SJ (1996) Multiple PEX genes are required for proper subcellular distribution and stability of Pex5p, the PTS1 receptor: evidence that PTS1 protein import is mediated by a cycling receptor. *J Cell Biol* 135:1763–1774.
37. Gonzalez KL, et al. (2017) Disparate peroxisome-related defects in *Arabidopsis pex6* and *pex26* mutants link peroxisomal retrotranslocation and oil body utilization. *Plant J* 92:110–128.
38. Rinaldi MA, et al. (2017) The PEX1 ATPase stabilizes PEX6 and plays essential roles in peroxisome biology. *Plant Physiol* 174:2231–2247.
39. Smith CE, et al. (2016) Spectrum of PEX1 and PEX6 variants in Heimler syndrome. *Eur J Hum Genet* 24:1565–1571.
40. Maxwell MA, Leane PB, Paton BC, Crane DI (2005) Novel PEX1 coding mutations and 5′ UTR regulatory polymorphisms. *Hum Mutat* 26:279.
41. Zhang Z, et al. (1999) Genomic structure and identification of 11 novel mutations of the *PEX6* (peroxisome assembly factor-2) gene in patients with peroxisome biogenesis disorders. *Hum Mutat* 13:487–496.
42. Muralla R, Lloyd J, Meinke D (2011) Molecular foundations of reproductive lethality in *Arabidopsis thaliana*. *PLoS One* 6:e28398.
43. Li XR, et al. (2014) *Arabidopsis* DAYU/ABERRANT PEROXISOME MORPHOLOGY9 is a key regulator of peroxisome biogenesis and plays critical roles during pollen maturation and germination in planta. *Plant Cell* 26:619–635.
44. Burkhart SE, Lingard MJ, Bartel B (2013) Genetic dissection of peroxisome-associated matrix protein degradation in *Arabidopsis thaliana*. *Genetics* 193:125–141.
45. Dirkx R, et al. (2005) Absence of peroxisomes in mouse hepatocytes causes mitochondrial and ER abnormalities. *Hepatology* 41:868–878.
46. Ratzel SE, Lingard MJ, Woodward AW, Bartel B (2011) Reducing *PEX13* expression ameliorates physiological defects of late-acting peroxin mutants. *Traffic* 12:121–134.
47. Zolman BK, Yoder A, Bartel B (2000) Genetic analysis of indole-3-butyric acid responses in *Arabidopsis thaliana* reveals four mutant classes. *Genetics* 156:1323–1337.
48. Woodward AW, Bartel B (2005) The *Arabidopsis* peroxisomal targeting signal type 2 receptor PEX7 is necessary for peroxisome function and dependent on PEX5. *Mol Biol Cell* 16:573–583.
49. Zolman BK, Monroe-Augustus M, Silva ID, Bartel B (2005) Identification and functional characterization of *Arabidopsis* PEROXIN4 and the interacting protein PEROXIN22. *Plant Cell* 17:3422–3435.
50. Monroe-Augustus M, et al. (2011) Matrix proteins are inefficiently imported into *Arabidopsis* peroxisomes lacking the receptor-docking peroxin PEX14. *Plant Mol Biol* 77:1–15.
51. Woodward AW, et al. (2014) A viable *Arabidopsis pex13* missense allele confers severe peroxisomal defects and decreases PEX5 association with peroxisomes. *Plant Mol Biol* 86:201–214.
52. Kao YT, Fleming WA, Ventura MJ, Bartel B (2016) Genetic interactions between PEROXIN12 and other peroxisome-associated ubiquitination components. *Plant Physiol* 172:1643–1656.
53. Hayashi M, et al. (2000) AtPex14p maintains peroxisomal functions by determining protein targeting to three kinds of plant peroxisomes. *EMBO J* 19:5701–5710.
54. Helm M, et al. (2007) Dual specificities of the glyoxysomal/peroxisomal processing protease Deg15 in higher plants. *Proc Natl Acad Sci USA* 104:11501–11506.
55. Zolman BK, Silva ID, Bartel B (2001) The *Arabidopsis pxa1* mutant is defective in an ATP-binding cassette transporter-like protein required for peroxisomal fatty acid β-oxidation. *Plant Physiol* 127:1266–1278.
56. Kao YT (2017) Insights from forward- and chemical-genetic studies on peroxisome functions, peroxisome-environment interactions, and the peroxisome-associated ubiquitination. PhD thesis (Rice University, Houston).
57. Lingard MJ, Monroe-Augustus M, Bartel B (2009) Peroxisome-associated matrix protein degradation in *Arabidopsis*. *Proc Natl Acad Sci USA* 106:4561–4566.
58. Li F, Vierstra RD (2012) Autophagy: a multifaceted intracellular system for bulk and selective recycling. *Trends Plant Sci* 17:526–537.
59. Young PG, Bartel B (2016) Pexophagy and peroxisomal protein turnover in plants. *Biochim Biophys Acta* 1863:999–1005.
60. Lai Z, Wang F, Zheng Z, Fan B, Chen Z (2011) A critical role of autophagy in plant resistance to necrotrophic fungal pathogens. *Plant J* 66:953–968.
61. Wang Y, Nishimura MT, Zhao T, Tang D (2011) ATG2, an autophagy-related protein, negatively affects powdery mildew resistance and mildew-induced cell death in *Arabidopsis*. *Plant J* 68:74–87.
62. Hänzelmann P, Schindelin H (2017) The interplay of cofactor interactions and post-translational modifications in the regulation of the AAA+ ATPase p97. *Front Mol Biosci* 4:21.
63. Pettersen EF, et al. (2004) UCSF Chimera–a visualization system for exploratory research and analysis. *J Comput Chem* 25:1605–1612.
64. Kao YT, Bartel B (2015) Elevated growth temperature decreases levels of the PEX5 peroxisome-targeting signal receptor and ameliorates defects of *Arabidopsis* mutants with an impaired PEX4 ubiquitin-conjugating enzyme. *BMC Plant Biol* 15:224.
65. Nuttall JM, Motley AM, Hettema EH (2014) Deficiency of the exportomer components Pex1, Pex6, and Pex15 causes enhanced pexophagy in *Saccharomyces cerevisiae*. *Autophagy* 10:835–845.
66. Kaur N, Zhao Q, Xie Q, Hu J (2013) Arabidopsis RING peroxins are E3 ubiquitin ligases that interact with two homologous ubiquitin receptor proteins(F). *J Integr Plant Biol* 55:108–120.
67. Pan R, Satkovich J, Hu J (2016) E3 ubiquitin ligase SP1 regulates peroxisome biogenesis in *Arabidopsis*. *Proc Natl Acad Sci USA* 113:E7307–E7316.
68. Lingard MJ, Bartel B (2009) *Arabidopsis* LON2 is necessary for peroxisomal function and sustained matrix protein import. *Plant Physiol* 151:1354–1365.
69. Farmer LM, et al. (2013) Disrupting autophagy restores peroxisome function to an *Arabidopsis lon2* mutant and reveals a role for the LON2 protease in peroxisomal matrix protein degradation. *Plant Cell* 25:4085–4100.
70. Goto-Yamada S, et al. (2014) Chaperone and protease functions of LON protease 2 modulate the peroxisomal transition and degradation with autophagy. *Plant Cell Physiol* 55:482–496.
71. Burkhart SE, Kao YT, Bartel B (2014) Peroxisomal ubiquitin-protein ligases peroxin2 and peroxin10 have distinct but synergistic roles in matrix protein import and peroxin5 retrotranslocation in *Arabidopsis*. *Plant Physiol* 166:1329–1344.
72. Haughn GW, Somerville C (1986) Sulfonylurea-resistant mutants of *Arabidopsis thaliana*. *Mol Gen Genet* 204:430–434.
73. Thole JM, Beisner ER, Liu J, Venkova SV, Strader LC (2014) Abscisic acid regulates root elongation through the activities of auxin and ethylene in *Arabidopsis thaliana*. *G3 (Bethesda)* 4:1259–1274.
74. Rinaldi MA, et al. (2016) The roles of β-oxidation and cofactor homeostasis in peroxisome distribution and function in *Arabidopsis thaliana*. *Genetics* 204:1089–1115.
75. Earley KW, et al. (2006) Gateway-compatible vectors for plant functional genomics and proteomics. *Plant J* 45:616–629.
76. Koncz C, Schell J (1986) The promoter of T_L-DNA gene 5 controls the tissue-specific expression of chimaeric genes carried by a novel type of *Agrobacterium* binary vector. *Mol Gen Genet* 204:383–396.
77. Clough SJ, Bent AF (1998) Floral dip: a simplified method for *Agrobacterium*-mediated transformation of *Arabidopsis thaliana*. *Plant J* 16:735–743.
78. Kunce CM, Trelease RN, Turley RB (1988) Purification and biosynthesis of cottonseed (*Gossypium hirsutum* L.) catalase. *Biochem J* 251:147–155.
79. Maeshima M, Yokoi H, Asahi T (1988) Evidence for no proteolytic processing during transport of isocitrate lyase into glyoxysomes in castor bean endosperm. *Plant Cell Physiol* 29:381–384.
80. Pracharoenwattana I, Cornah JE, Smith SM (2007) *Arabidopsis* peroxisomal malate dehydrogenase functions in β-oxidation but not in the glyoxylate cycle. *Plant J* 50: 381–390.